JOURNAL OF MATERIALS SCIENCE 5 (1970) 901-908

Clustering in Fe–Mo Alloys

T. ERICSSON
Aktiebolaget Volvo, Gothenburg, Sweden

S. MOURIKIS
Department of Physics, University of Athens, Athens, Greece

J. B. COHEN
Department of Materials Science, Northwestern University, Evanston, Illinois, USA

A quantitative study was made of the diffuse scattering due to clustering at 550° C in an Fe–6.1 at. % Mo alloy. The intensity due to local order was separated from the effects of different atomic sizes of the species and first-order thermal diffuse scattering, making use of the symmetry of these contributions. The Warren local-order parameters have been derived and used in a computer program to generate the corresponding atomic distributions. Comparison of the atomic configurations for clustering in this alloy are made with those for our previous measurements on a more dilute alloy, Fe–3.9 at. % Mo at the same ageing temperature.

In both alloys there are irregularly shaped Mo-rich clusters, but these are very dilute. For the smallest clusters there is some resemblance to the equilibrium precipitate Fe_2Mo. This weak Mo concentration in these zones explains why previous investigators have found little hardening due to GP zones in this alloy. Also, the average displacement of Fe atoms from lattice sites is less in the alloy of 6.1 at. % Mo than in the more dilute alloy; this suggests there may be a relationship of these displacements to alloy-softening.

The available Mössbauer spectra for this alloy are re-examined, and the suggested assignment of the Fe peaks to specific numbers of Mo neighbours in the first two shells is revised on the basis of the computer-generated atomic configurations; the third neighbour shell appears to be important.

1. Introduction

In quenched iron-rich Fe–Mo alloys containing 20 at. % Mo, Mo-rich clusters form as discs on dislocations [1], if ageing is carried out at 500° C. After long ageing times these discs form Mo-rich particles. Above this temperature, only discontinuous precipitation occurs. The precipitate is Fe_3Mo_2, although below 900° C the equilibrium phase should be Fe_2Mo [1]. For a more dilute alloy containing 6 at. % Mo, in a study of the Mössbauer spectrum by Marcus, Fine, and Schwartz [2], quenched alloys exhibited two "satellites" near each of the six resonant absorption bands due to iron; the quenched alloy is not random. The pattern was interpreted as due to Fe atoms with 0, 1, or 2 Mo atoms among their 14 nearest neighbours. At 650° C, these distributions do not change until Fe_2Mo forms, when the number of Fe atoms with 2 Mo neighbours falls. At 550° C, for 2 to 30 h, there is a decrease in the number of these atoms, then an increase, and finally Fe_2Mo appears. This change in the number of Fe atoms with two neighbours was interpreted as due to the formation of Mo atom clusters (which decreases the Fe atoms with Mo neighbours) followed by the formation of Fe_2Mo. Preliminary X-ray studies performed by us and reported in [2] showed weak diffuse scattering near Bragg peaks after quenching; the intensity increased for 5 h at 550° C and then decreased when Fe_2Mo formed.

In this paper, we present results of a detailed, quantitative study of the X-ray scattering from a single crystal. The new experimental techniques and methods that were employed have been described by us in detail [3]. Briefly these

methods allow a separation of the contributions to scattering of local order (clustering or short-range order) from those due to differences in atomic size or thermal vibrations, with measurements at only one temperature, following a procedure outlined by Sparks and Borie [4, 5]; the method is based on the different symmetries in reciprocal space of the various contributions. Heretofore, quantitative measurements could only be made on alloys with short-range order. In our previous paper [3] the methods were tested with Fe–3.9 at. % alloy. We shall examine the results on that alloy as well as the new results on Fe–6.1 at. % Mo presented here, to provide a more complete description of clustering in this system.

With the Warren local-order parameters obtained from the diffuse scattering, "pictures" of the alloy system have been obtained; the computer simulation developed by Gehlen and Cohen [6] was employed to obtain the atomic configurations compatible with these parameters. These will be examined qualitatively and quantitatively, and compared with the data from the Mössbauer investigation, and with studies of age-hardening [7]. Finally, the displacements of atoms from lattice sites may be related to the alloy-softening that occurs in this system [7].

2. Experimental Details

Because all the details of the measurements on the alloy of 3.9 at. % were carefully noted in [3], we give details only for the alloy of 6.1 at. % Mo.

2.1. Sample Preparation

For the 6.1 at. % Mo, the starting material was a 1.3 cm thick sheet of nominal composition 9.92 wt % Mo, 0.022 wt % C, 0.0032 wt % N, the rest being Fe. After all the heat-treatments to be described, the composition of the specimen was measured by X-ray fluorescence and found to be 6.06 $\pm$ 0.15 at. % Mo. A strip was cut from this sheet and alternately cold-rolled and recrystallised (in a vacuum induction furnace) at about 1300° C until a final grain size of about 15 mm was obtained. A large grain was cut out with a diamond wheel and ground so that the surface normal was within $\frac{1}{2}$° of a $\langle 101 \rangle$ direction. The specimen was vacuum-annealed at 1050° C for 1 h, quenched into iced brine, reannealed 5 h at 550° C and slowly cooled (about 1.5° C/sec) to room temperature.* This treatment was chosen to correspond to that which brought about a decrease in Fe atoms with 2 Mo neighbours, as found in [2]. The crystal was then mechanically polished followed by electropolishing to remove any surface deformation. (This was checked with Laue patterns.) A light chemical etch was applied to reveal any grain-boundaries. Fe-fluorescence from the specimen produced by incident CuK_α was constant for 2θ larger than 20°, indicating negligible surface irregularities [9].

(A large single crystal was employed in the study of Fe–3.9 at. % Mo; see [3].)

2.2. Measurements

The measurements were made with a GE XRD-5 diffractometer equipped with GE electronics, a proportional counter, pulse-height analyser and CoK_α radiation, monochromated with a doubly bent LiF crystal. The specimen was mounted on a small goniometer for fine adjustments. This was attached to the standard GE-quarter-circle eucentric goniometer. The sample and the small goniometer were surrounded by a plastic bag filled with flowing He. With an initial orientation, $\chi = 90°$, the [101] direction was adjusted parallel to the diffraction plane. (For the alloy of 3.9 at. % Mo, the sample was in a vacuum.)

The divergence and receiving slits were set to correspond to a resolution of 0.04 reciprocal space units at the middle of the 2θ range explored. The background was measured using a lead trap in the sample position. For 14 data points with 2θ between (the minimum) 29.5° and 37° the He-filled bag could not be used owing to scattering from the bag; the background due to air-scattering ranged between 42% and 29% of the measured total intensity in this region.† Between 37° 2θ and 67° 2θ, using the He-filled bag, the background was only a few per cent. of the total. Between 67° 2θ and 151° 2θ measurements were again made in air because the background was still small. For 10 data points with 2θ between 151° and the maximum value 153°, no receiving scatter slit could be used owing to the geometry of the experimental arrangement. The

*According to the estimates in [8], this cooling rate for these alloys is sufficient to prevent any appreciable atomic rearrangement; the results are thus characteristic of the heat-treatment at 550° C.

†The high background due to air-scattering for these points with 2θ lower than 37° causes a high degree of uncertainty in the corresponding data. This is not serious, however, because these are all low intensity points far from a Bragg peak. The measurements on the Fe-3.9 at. % alloy made in vacuum [3] revealed no fine details in this region.

background was then about 6 to 19% of the measured intensity.

The absorption in the plastic bag was 11% without He and 8.7% with He. The length of the beam path through the bag and thus the X-ray absorption varied slightly with 2θ and χ; this was accounted for in an absorption correction of the data points.

The Co tube was operated at 45 kV; therefore, the measured intensity had to be corrected for Fe-fluorescence from $\lambda/2$ and $\lambda/3$ in the crystal-monochromated beam. Since the voltage was the same as in the earlier work [1] it was assumed that the fluorescent intensity per unit beam power and per at.% Fe was the same as before. The estimated Fe fluorescence amounted to typically 30% of the measured intensity. Thus, approximately half the recorded intensity corresponded to parasitic scattering from air or He, and fluorescence.

(The measurements on the alloy of 3.9 at.% Mo being made in vacuum, these corrections were much less significant.)

The direct beam intensity was measured using the same technique as in our earlier paper [3]. The intensity decreased from 0.43×10^8 cps to 0.41×10^8 cps during the experiment, but one data point was measured regularly and the measured intensity was corrected for this drift. (The monitor counter, used for Fe–3.9 at. % Mo, was not employed here.) The transformation of the measured intensity to electron units per atom was also performed in the same way as before, and Compton scattering [10] was subtracted to obtain the coherently scattered intensity.

3. Results

3.1. Atomic Distributions

The total diffuse intensity observed for the present alloy is similar to that described in our earlier paper, with the maxima of the diffuse intensity at the fundamental peaks. However, the streaks of high intensity extending from the 101 and 211 peaks were not found for this alloy. The distribution of the local-order intensity is not very different from the one found in the 3.9 at. % alloy, which was essentially spherically distributed around the Bragg peaks. (The streaks observed in that alloy were due to size effect modulation and Huang scattering plus TDS.) Thus no plots of the intensity distribution in reciprocal space are given here.

The local-order parameters α_i derived from the local-order intensity are given in table I both corrected (column 2), and not corrected (column 1), for the variation with $\sin\theta/\lambda$ of the scattering factors (see our earlier paper for details on this correction). The α_0 terms are slightly larger than the ones found for the Fe–3.9 at.% Mo alloy, indicating more uncorrected parasitic scattering in the present case, which is to be expected owing to the less refined technique used. Column 3 presents the results obtained by subtracting the indicated value (an assumed constant but undetected background) to bring α_0 to its theoretical value of unity. The value is not

TABLE I Warren local-order parameters α_i for Fe–6.1 at.% Mo.

Co-ordination shell i	lmn	1 uncorrected	2 corrected for variation in scattering factors over volume of measurement	3 0.46 cps removed*
0	000	1.328	1.255	1.000
1	111	0.093	0.071	0.069
2	200	0.060	0.043	0.042
3	220	0.034	0.024	0.024
4	311	0.030	0.022	0.022
5	222	0.035	0.027	0.028
6	400	0.027	0.020	0.019
7	331	0.018	0.013	0.013
8	420	0.018	0.014	0.014
9	422	0.012	0.009	0.009
10′	511	0.012	0.008	0.008
10″	333	0.011	0.009	0.009
11	440	0.007	0.007	0.007
12	531	0.008	0.007	0.007

*8% of a typical data point

TABLE II Conditional pair probabilities, $P_j^{Mo}|_k^{Mo}$ and average numbers of Mo atoms around an Mo atom.

Shell	Co-ordination number	3.9 at. % Mo				6.1 at. % Mo		
		lmn	$P_j^{Mo} \mid_k^{Mo}$	average no. Mo atoms		$P_j^{Mo} \mid_k^{Mo}$	average no Mo atoms	
				actual	random		actual	random
1	8	111	0.132	1.06	0.31	0.126	1.21	0.49
2	6	200	0.080	0.48	0.23	0.100	0.60	0.37
3	12	220	0.080	0.96	0.47	0.084	1.07	0.73
4	24	311	0.065	1.56	0.94	0.082	1.97	1.46
5	8	222	0.070	0.56	0.31	0.087	0.70	0.49
6	6	400	0.073	0.44	0.23	0.079	0.47	0.37

unreasonable, being of the order of 8% of a typical data point.

The definition of the Warren local-order parameters is:

$$\alpha_{lmn} = 1 - P_j^A \mid_k^B / X_A \qquad (1)$$

where *lmn* are co-ordinates of the interatomic vector between sites j and k, X_A is the mole fraction of element A and $P_j^A \mid_k^B$ is the conditional probability that there is an A atom at site j if there is a B atom at k. (Instead of the co-ordinates *l*, *m*, *n* the shell number *i* is often used.) Putting A = Fe and B = Mo and noting that

$$P_j^A \mid_k^B + P_j^B \mid_k^B = 1\,,$$
$$P_j^{Mo} \mid P_k^{Mo} = X_{Fe} \cdot \alpha_{lmn} + X_{Mo}\,. \qquad (2)$$

The number of Mo atoms around an Mo atom in a shell with co-ordination number Z is then $Z(X_{Fe} \cdot \alpha_{lmn} + X_{Mo})$. In table II this quantity is given for both the Fe–6.1 at. % Mo and Fe–3.9 at. % Mo alloys.* The six first α's for the 6.1 at. % Mo alloy are all smaller than for the 3.9 at. % Mo alloy but the number of Mo atoms in a shell around any Mo atom is greater. The random values are also given. The excess in each shell over the random value is about the same for both alloys.

The atomic configurations that satisfy the measured local order parameters, α_1, α_2, and α_3, were developed for 3D models of 16 000 atoms, using an extended version of the Gehlen-Cohen approach [6] developed by J. E. Gragg, Jr [11]. (It is capable of handling fcc or bcc and up to 108 000 atoms.) The α's in column 1 and 3 of table I and the α's corresponding to a random distribution ($\alpha_1 = \alpha_2 = \alpha_3 = 0$) were employed. Fig. 1 shows the distribution of neighbours of a Mo atom for both alloys. (Note how well the computer-generated random alloys agree with the calculated random distribution.) Fig. 2 shows

TABLE III Characterisation of atomic configurations generated by Computer: maximum, median, and average cluster sizes and average Mo concentration in clusters with 8 to 18 Mo atoms and with more than 18 Mo atoms, Fe–3.9 at. % Mo and Fe–6.1 at. % Mo.

	Maximum cluster size number of Mo atoms		Median cluster size number of Mo atoms		Average cluster size* number of Mo atoms		Average Mo concentration in at. % of clusters with			
							8–18 Mo atoms		> 18 Mo atoms	
	3.9 at. %	6.1 at. %	3.9 at. %	6.1 at. %	3.9 at. %	6.1 at. %	3.9 at. %	6.1 at. %	3.9 at. %	6.1 at. %
Uncorrected†	29	66	7	12	7.9	11.0	12.0	12.3	8.6	5.7
Corrected‡ to $\alpha_0 = 1$	39	66	6	9	7.6	11.0	10.8	12.5	6.8	7.7
Random	11	31	2	4	4.5	7.2	7.1	8.0		5.8

*Single Mo atoms and pairs of Mo atoms were excluded when calculating the average size.

†Configuration generated with α_1, α_2, and α_3 taken from column 1, table I in this paper and column 1, table II in our earlier paper [1].

‡Configuration generated with α_1, α_2, and α_3 taken from column 3, table I in this paper and column 4, table II in our earlier paper [1].

*The sets of α's that have been used are those for which α_0 was adjusted to unity after the local order intensity was corrected for the $\sin\theta/\lambda$ variation of the scattering factor terms; that is column 4 of table I of our earlier paper [3] and column 3 of table I here.

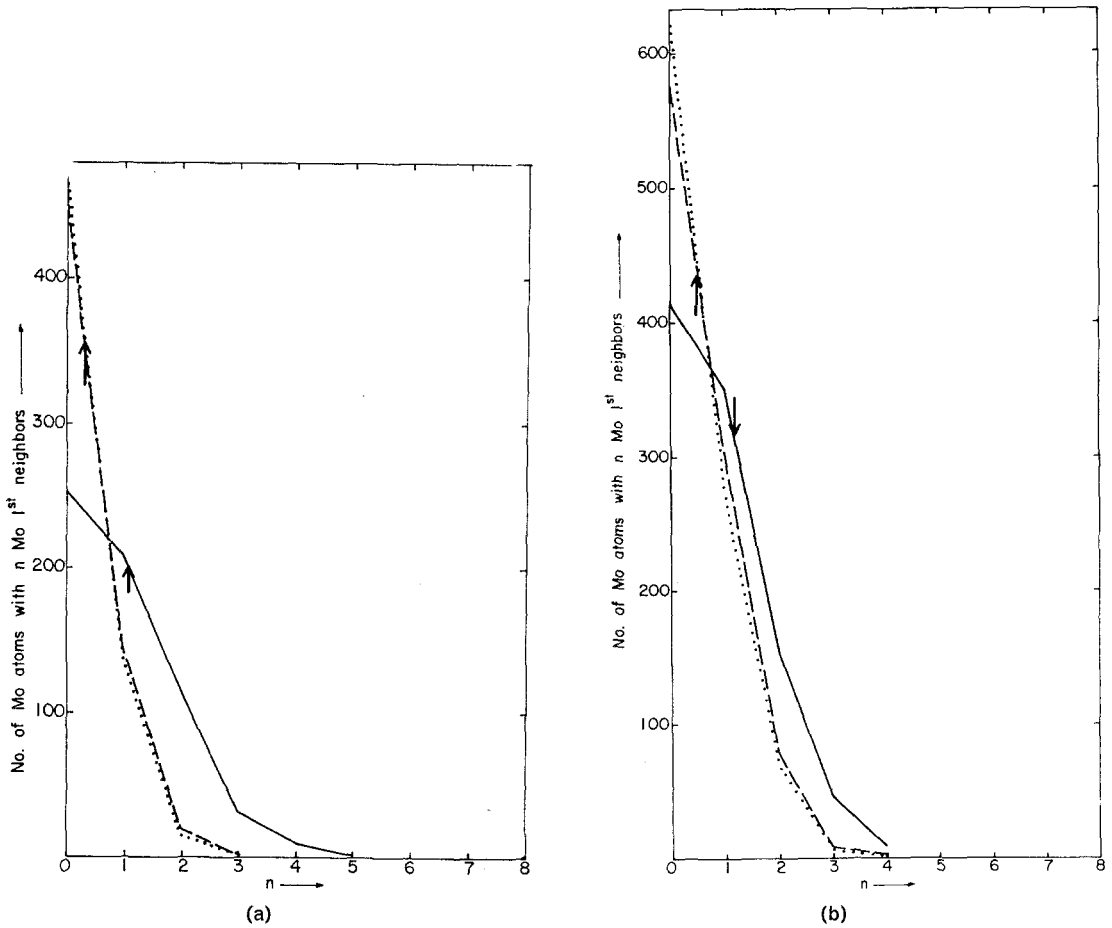

Figure 1 The number ($N_{Mo}{}^{n}$) of Mo atoms having n Mo first neighbours. ——— actual alloy; ..... random alloy (computer); — — — theoretical for a random alloy:

$$N_{Mo}{}^{n} = X_{Mo}\, 16000\, (X_{Fe})^{8-n} (X_{Mo})^{n} \binom{n}{8}$$

Arrows indicate the values obtained from α_i (a) 3.9 at. % Mo; (b) 6.1 at. % Mo.

for Fe–6.1 at. % Mo how many Mo atoms belong to clusters below a size indicated on the abscissa, for the three sets of α's. An Mo atom was considered part of a cluster if it was a first, second, or third nearest neighbour of at least one other Mo atom. As expected, the larger the α's, the more Mo atoms are in large clusters. A similar figure for the 3.9 at. % alloy was presented by us in [3]. The maximum cluster sizes, the median cluster sizes as defined in fig. 1 and the average cluster sizes excluding single Mo atoms and pairs are given in table III for both alloys. The clusters were all irregular in shape; see fig. 3 for two examples. If a cluster is inscribed in a box with its edges parallel to the unit cell edges, an average Mo concentration can be calculated for the cluster. Table III also gives this average for all clusters with 8 to 18 Mo atoms and with more than 18 Mo atoms.

The average Mo content of clusters with 8 to 18 Mo atoms is only slightly larger for the 6.1 at. % Mo alloy than for the 3.9 at. % Mo alloy. The same is true for regions with the maximum Mo content (not shown in table III), which is 22 at. % for the 6.1 at. % Mo alloy and 20 at. % for the 3.9 at. % Mo alloy. These concentrations approach the value of 33 at. % Mo corresponding to the phase Fe_2Mo, which is precipitated in both alloys after longer annealing times at 550°C. It is the smaller clusters that have this concentration. Considering that atoms in the surface of such regions could not have exact Fe_2Mo surroundings, this is some indication that nuclei of this phase exist prior to precipitation. In fig. 3 there is alignment of Mo nearest-neighbour atoms along ⟨110⟩ directions in all three projections and there tend to be two adjacent directions like this, often with Fe atoms between

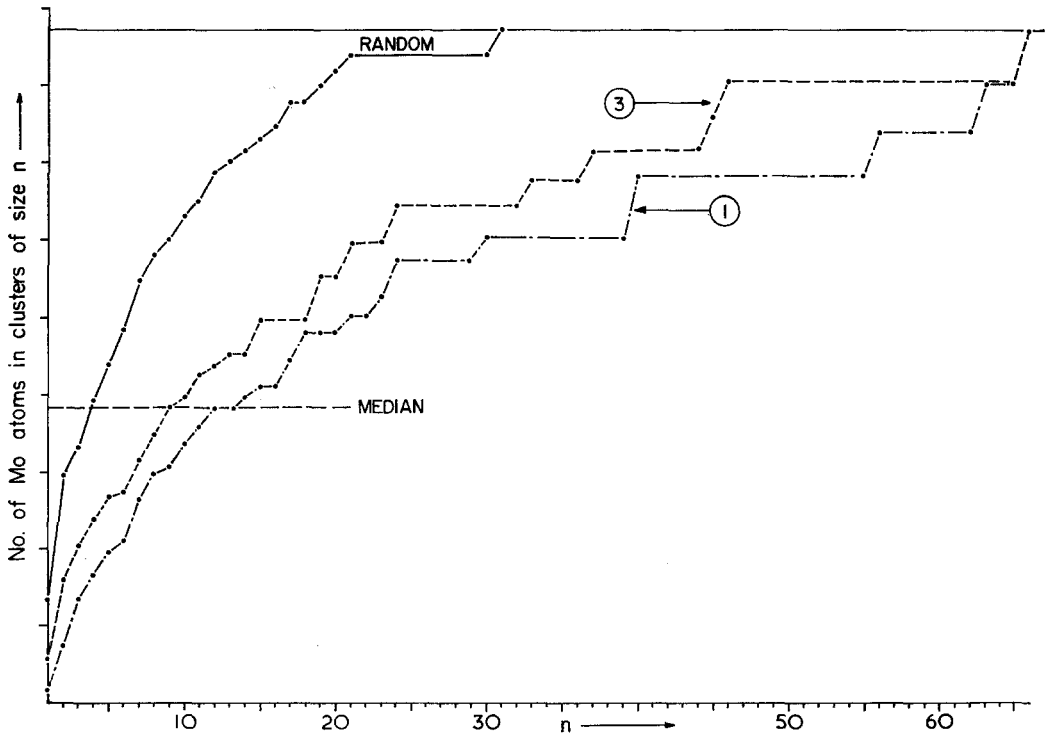

Figure 2 The distribution of Mo atoms over clusters of various sizes, Fe–6.1 at. % Mo. The ordinate indicates the number of Mo atoms in clusters below the size given on the abscissa. The circled numbers refer to the columns in table I which were the input to the computer.

Mo along each row. (These rows are evident also in individual planes of a cluster.) Fe_2Mo is a $MgZn_2$ Laves phase (Strukturbericht C14) with alternate double simple hexagonal layers of Fe and Mo, the double layers stacked in an hcp sequence. When it precipitates from this alloy the basal plane is parallel to {1 1 0} planes of the Fe-rich bcc phase [12]; such a structure involves exactly these kinds of rows relative to the matrix.

The median and average cluster sizes are approximately proportional to the Mo content. Thus, the larger number of Mo atoms in the 6.1 at. % alloy is achieved by a larger number of clusters and by larger sizes of clusters, not by a higher concentration of Mo atoms within the clusters.

The results in the second row of table III are included to show that this analysis is not sensitive to small errors in the α's.

(The atomic configurations were generated using only α_1, α_2, α_3. The computer program can also calculate higher order α's from the generated configuration to compare with experiment. These were of the same sign as the measured values but generally smaller by a factor of about five.)

3.2. Static Displacements of Fe atoms

The separated scattering due to size differences of the atoms was analysed in the same way for the 6.1 at. % Mo alloy as for the 3.9 at. % Mo alloy (see [3]). Table IV gives the length of the average displacement vector $\delta_{lmn}{}^{\mathrm{FeFe}}$ and its angle with the vector $\langle l, m, n\rangle$ for both alloys. (These terms are obtained from the modulation of diffuse intensity due to size effects.) The average displacements for all shells except the second one are smaller than for the 3.9 at. % Mo alloy; the first value is about 20 % of that for the more dilute alloy. The largest value is only about 0.2 % of the smallest interatomic distance.

4. Discussion

In [7] it was shown that heat-treatment to produce only clustering did not appreciably alter the mechanical properties of the 6 at. % Mo alloy. The reason for this is now clear; the vast majority of zones are indeed very dilute. Dislocations would not produce much interfacial energy on cutting through such regions. It is also interesting to note that the average displacement of Fe atoms from lattice sites is much smaller in

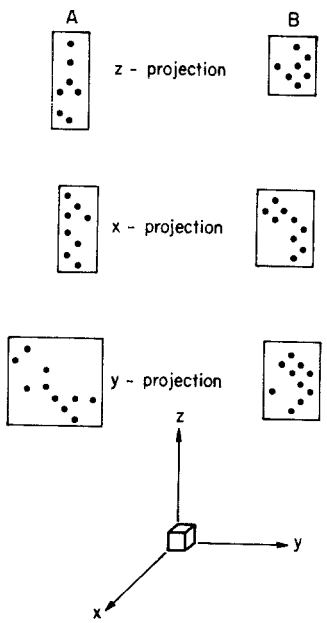

Figure 3 Projections along the three unit cell edges of two clusters with 11 Mo atoms, Fe – 6.1 at. % Mo.

Fe–6.1 at. % Mo than in 3.9 at. % Mo. Alloy-softening is much less pronounced in the former alloy than in the latter. The reduction in the average displacement in the 6.1 at. % Mo alloy appears to be due to the larger number and size of the clusters; both alloys have about the same fraction of Mo atoms with no Mo first neighbours. While the reason for alloy-softening is still controversial, these results suggest that it may be the reduction of the Peierls stress rather than "scavenging" in this system; further studies of the displacements in other systems are warranted.*

It is interesting to speculate on the nucleation event for Fe_2Mo. Our results indicate that small zones resemble the composition and the structure of this equilibrium phase. The reason for the long incubation time for precipitation in this system is thus not clear.

Finally, in table Va, we compare the results from the computer-generated configurations with those from the interpretation of the peaks in the Mössbauer spectra [2]. While there is no question from the position of the peaks in this pattern that the one identified as due to iron atoms with the least number of Mo neighbours is correctly chosen, the assumption in [2] that it is due to a specific number (none) in only the first two neighbour shells is quite arbitrary, as is also true of the other peaks detected in the pattern and listed in table V. In fact, a comparison of columns 2 and 4 show that the manner in which the pattern was interpreted implies a *decrease* from random in the number of Fe atoms with no Mo neighbours in the first two shells; this is the reverse of what one would expect for clustering. The agreement with the computer maps is not good. The agreement for the other peaks is also poor! At this point, with one of the investigators in the Mössbauer study, Professor L. H. Schwartz, we considered a possible role of third neighbours to an Fe atom, particularly those groups that had no Mo neighbours in the first three shells, or 1, or 2 Mo atoms. In table Vb we show that in fact such an interpretation fits the data much more closely. (About 20% of the Fe atoms were not included in the groupings mentioned. The theoretical fractions and those from the computer maps represent the fractions of the population counted, not the fraction of

TABLE IV The average displacement between two Fe atoms, δ^{Fe-Fe} (Å), and the direction of this displacement, ϕ relative to the interatomic vector l_{mmi}.

Shell, i	lmn	Fe–3.9 at. % Mo		Fe–6.1 at. % Mo	
		$\lvert\delta^{FeFe}\rvert$	ϕ (°)	$\lvert\delta^{FeFe}\rvert$	ϕ (°)
1	111	0.0022	180	0.0004	180
2	200	0.00005	180	0.0009	0
3	220	0.0010	0	0.0003	0
4	311	0.0006	10	0.0004	148
5	222	0.00005	0	0.0004	0
6	400	0.0006	180	0.0003	180
7	331	0.0007	156	0.0003	162
8	420	0.0003	165	0.0001	117

*The techniques are presented in [3]. It is worth stating here that what one measures is the average static displacement. From peak depressions in alloys it is well known that one can measure the root-mean-square displacements [4]. While these are often assumed to be the same thing, this is not really the case, and the former may be of more interest.

TABLE V Comparison of atomic distributions with interpretation of Mössbauer spectra in [2], for Fe–6.1 at.% Mo.

(a)

Fraction of Fe atoms with indicated number of Mo neighbours in 1st and 2nd shell	Random (calculated)	Clustered from computer simulation	From [2]
0	0.438	0.498	0.384
1	0.402	0.296	0.561
2	0.160	0.133	0.055
> 2	—	0.072	—

(b)

Fraction of Fe atoms with indicated number of Mo atoms in 1st three shells	Random (calculated)	Clustered from computer simulation	From [2]
0	0.25	0.36	0.384
1 or 2 (with 1 in each of two shells).	0.64	0.55	0.561
2 in either 1st, 2nd, or 3rd shell	0.11	0.09	0.055

total Fe atoms as was the case for the fractions in a. This corresponds more closely to the situation in the Mössbauer experiment. Normalising the values in a would have made the comparison even worse.)

It is worth emphasising that it is the agreement of the Mössbauer experiment with the fraction of Fe atoms with no Mo neighbours in the first three shells (from the computer maps) that is most important; this peak in the spectrum is clearly due to Fe atoms with a minimum number of Mo neighbours, while the others might be due to several possible Mo neighbour distributions other than the ones we chose. Note also that the value for this first peak, both in the computer simulation and in the Mössbauer spectra, is now *higher* than the random value, as is expected for clustering.

The need for the computer maps in understanding the Mössbauer spectra in alloys is clear in this case and more detailed studies along these lines should prove interesting.

Acknowledgements

This work was supported by ARPA through Northwestern University's Materials Research Center and by NSF. One of the authors (T.E.) was partially supported by AB Atomenergi, Stockholm, Sweden, and thanks are due to this company for permission to use its computer facilities. The assistance of Mr H. Berg and Mr P. Bardhan in making and analysing the computer runs of the atomic distribution is gratefully acknowledged. Discussion of the Mössbauer patterns with Professor L. H. Schwartz and about the strengthening with Professor M. E. Fine were stimulating.

References

1. E. HORNBOGEN, *J. Appl. Phys.* **32** (1961) 135.
2. H. L. MARCUS, M. E. FINE, and L. H. SCHWARTZ, *ibid* **38** (1967) 4750.
3. T. ERICSSON and J. B. COHEN, *Acta Cryst.* (in press).
4. C. J. SPARKS and B. BORIE, in "Local Atomic Arrangements Studied by X-Ray Diffraction", edited by J. B. Cohen and J. E. Hilliard (Gordon and Breach, New York, 1966).
5. B. BORIE, and C. J. SPARKS (to be published in *Acta Cryst.* 1970).
6. P. C. GEHLEN and J. B. COHEN, *Phys. Rev.* **139** (1965) A844.
7. A. URAKAMI, H. L. MARCUS, M. MESHII, and M. E. FINE, *Trans. ASM* **60** (1967) 344.
8. B. MOZER, D. T. KEATING, and S. C. MOSS, *Phys. Rev.* **175** (1968) 868.
9. P. M. DE WOLFF, *Acta Cryst.* **9** (1956) 682.
10. International Tables for X-Ray Crystallography, Vol. III (The Kynoch Press, Birmingham, 1962).
11. J. E. GRAGG, JR., PhD Thesis, Northwestern University, Evanston, Illinois, 1970.
12. A. URAKAMI, MS Thesis, Northwestern University, Evanston, Illinois, 1966.

Received 21 May and accepted 16 June 1970.